BULLETIN OF THE POLISH ACADEMY OF SCIENCES
TECHNICAL SCIENCES, Vol. 72(4), 2024, Article number: e150332
DOI: 10.24425/bpasts.2024.150332

The discrete, fractional order model of a two-dimensional temperature field using Grünwald-Letnikov definition

Krzysztof OPRZĘDKIEWICZ*

AGH University of Science and Technology, al. A. Mickiewicza 30, 30-059 Kraków, Poland

Abstract. In the paper a new, fractional order, discrete model of a two-dimensional temperature field is addressed. The proposed model uses Grünwald-Letnikov definition of the fractional operator. Such a model has not been proposed yet. Elementary properties of the model: practical stability, accuracy and convergence are analysed. Analytical conditions of stability and convergence are proposed and they allow us to estimate the orders of the model. Theoretical considerations are validated using experimental data obtained with the use of a thermal imaging camera. Results of analysis supported by experiments point that the proposed model assures good accuracy and convergence for low order and relatively short memory length.

Keywords: fractional order systems; heat transfer equation; fractional order state equation; Grünwald-Letnikov definition; practical stability; accuracy; convergence; thermal camera.

1. INTRODUCTION

Non-integer order or fractional order (FO) models of different physical phenomena have been presented by many authors for years. Fundamental results can be found e.g. in books and papers [1–3] (the heat transfer in an one dimensional beam), [4] (fractional models of chaotic systems and ionic polymer metal composites, among others). FO models of diffusion processes are proposed by [5–7]. Results using new Atangana-Baleanu operator are collected in [8]. This paper presents also the use of FO approach to express of the FO blood alcohol model, the Christov diffusion equation and fractional advection-dispersion equation for groundwater transport processes.

Recently FO models are used to describe a spread of diseases, among other things. This issue is considered e.g. in the papers given by [9] (the modeling of the dynamics of COVID using Caputo-Fabrizio operator), [10] (the modeling of a transmission of Zika virus using Atangana-Baleanu operator).

The state space FO models of the one dimensional heat transfer have been proposed in many previous papers of author, e.g. [11–18]. These models used different FO operators: Grünwald-Letnikov, Caputo, Caputo-Fabrizio and Atangana-Baleanu as well as discrete operators: continuous fraction expansion (CFE) and fractional order backward difference (FOBD). Each model has been thoroughly theoretically justified and validated using experimental results. In addition, each of them assures better accuracy in the sense of square cost function than its IO analogue.

The time-continuous, two-dimensional generalization of FO models mentioned above is proposed in the papers [19, 20]. A discrete-time, FO model of this class of thermal processes has no been proposed yet.

Models of temperature fields obtained with the use of thermal cameras are discussed, e.g. in papers: [21, 22]. Analytical solution of a two-dimensional, IO heat transfer equation is presented in the paper [23]. Numerical solving of partial differential equations has been discussed in many books (see e.g. [24]). Fractional Fourier integral operators are analyzed by [25]. It is important to note that a significant part of known investigations deals only with a steady-state temperature fields with omitting their dynamics.

This paper presents a new, discrete time model of the heat transfer in the thin, two-dimensional metallic surface. The model uses the fractional order backward difference (FOBD) to describe the fractional operator. Such a model has not been proposed yet. The model is proposed and analysis of its basic properties: practical stability, accuracy and convergence is given. Theoretical considerations are verified by experimental results.

The organization of the paper is following. Firstly elementary ideas and definitions from fractional calculus are given. Next the experimental heat system and its time-continuous model are recalled. As the main result the discrete model using FOBD is proposed and its basic properties: practical stability, accuracy and convergence are discussed. Then parameters of the model are numerically identified using data from real experimental system and IAE cost function. Finally the practical stability, accuracy and convergence of the identified model are examined.

*e-mail: kop@agh.edu.pl

Manuscript submitted 2024-02-23, revised 2024-04-05, initially accepted for publication 2024-04-26, published in July 2024.

2. PRELIMINARIES

2.1. Basics of fractional calculus

Theoretical preliminaries of the fractional calculus can be found in many books, e.g. in the section "Fractional Systems: Theoretical Foundations" of [26].

The non-integer-order, integro-differential operator is defined as follows (see e.g. [1, 2, 26–28]):

Definition 1. (The elementary non-integer order operator) The non-integer-order integro-differential operator is defined as follows:

$$ {}_aD_t^{\alpha} f(t) = \begin{cases} \dfrac{\mathrm{d}^{\alpha} f(t)}{\mathrm{d}t^{\alpha}} & \alpha > 0, \\ f(t) & \alpha = 0, \\ \displaystyle\int_a^t f(\tau)(\mathrm{d}\tau)^{\alpha} & \alpha < 0, \end{cases} \tag{1} $$

where a and t denote time limits for operator calculation, $\alpha \in \mathbb{R}$ denotes the non-integer order of the operation. If $\alpha \in \mathbb{Z}$, then the operator (1) turns to classic integer order operator.

The fractional-order, integro-differential operator can be described by definitions given by Grünwald and Letnikov, Riemann and Liouville (RL) and Caputo (C). In this paper the C and GL definitions are employed (see e.g. [2], [27], [28], [1]), [29]):

Definition 2. (The Caputo definition of the FO operator)

$$ {}_0^C D_t^{\alpha} f(t) = \frac{1}{\Gamma(M-\alpha)} \int_0^{\infty} \frac{f^{(M)}(\tau)}{(t-\tau)^{\alpha+1-M}} \mathrm{d}\tau, \tag{2} $$

where $M-1 < \alpha < M$ is the fractional order of operation and $\Gamma(..)$ is the Gamma function.

Definition 3. (The Grünwald-Letnikov definition of the FO operator)

$$ {}_0^{GL} D_t^{\alpha} f(t) = \lim_{h \to 0} h^{-\alpha} \sum_{l=0}^{[\frac{t}{h}]} (-1)^l \binom{\alpha}{j} f(t-lh). \tag{3} $$

In (3) $\binom{\alpha}{l}$ is a binomial coefficient into real numbers:

$$ \binom{\alpha}{l} = \begin{Bmatrix} 1, & l = 0 \\ \dfrac{\alpha(\alpha-1)\ldots(\alpha-l+1)}{l!}, & l > 0 \end{Bmatrix}. \tag{4} $$

The GL definition is limit case for $h \to 0$ of fractional order backward difference, commonly employed to discrete FO calculations:

Definition 4. (The fractional order backward difference)

$$ (\Delta^{\alpha} x)(t) = \frac{1}{h^{\alpha}} \sum_{l=0}^{L} (-1)^l \binom{\alpha}{l} x(t-lh). \tag{5} $$

Denote coefficients $(-1)^l \binom{\alpha}{l}$ by d_l:

$$ d_l = (-1)^l \binom{\alpha}{l}. \tag{6} $$

The coefficients (6) can be also calculated with the use of the following, equivalent recursive formula (see e.g. [4], p. 12), useful in numerical calculations:

$$ \begin{aligned} d_0 &= 1, \\ d_l &= \left(1 - \frac{1+\alpha}{l}\right) d_{l-1}, \quad l = 1, \ldots, L. \end{aligned} \tag{7} $$

It is proven in [30] that:

$$ \sum_{l=1}^{\infty} d_l = 1 - \alpha. \tag{8} $$

From (7) and (8) it can be seen at once that:

$$ \sum_{l=2}^{\infty} d_l = 1. \tag{9} $$

In (5) L denotes a memory length necessary to correct approximation of a non-integer order operator. Unfortunately good accuacy of PSE approximation requires the use of high value of L which can make difficulties in implementation.

The discrete, fractional order state equation using definition (5) is written as follows (see for example [31]):

$$ \begin{cases} (\Delta_L^{\alpha} x)(t+h) = A^+ x(t) + B^+ u(t), \\ y(t) = C^+ x(t), \end{cases} \tag{10} $$

where $x(t) \in \mathbb{R}^N$ is the state vector, $u(t) \in \mathbb{R}^P$ is the control, $y(t) \in \mathbb{R}^M$ is the output. A^+, B^+ and C^+ are state, control and output matrices respectively. If we shortly denote k-th time instant: hk by k, then equation (10) turns to (see e.g. [32]):

$$ \begin{cases} (\Delta_L^{\alpha} x)(k+1) = A^+ x(k) + B^+ u(k), \\ y(k) = C^+ x(k), \end{cases} \tag{11} $$

where:

$$ A^+ = h^{\alpha} A, \tag{12} $$

$$ B^+ = h^{\alpha} B, \tag{13} $$

$$ C^+ = C. \tag{14} $$

The solution of state equation (11) takes the form:

$$ x(k+1) = P^+ x(k) - \sum_{l=2}^{L} A_l^+ x(k-l) + h^{\alpha} B^+ u(k), \tag{15} $$

where:

$$ P^+ = A^+ + \alpha I, \tag{16} $$

$$ A_l^+ = d_l I_{N \times N}. \tag{17} $$

2.2. The practical stability

An idea of the practical stability needs to be recalled next. It was proposed by Kaczorek in [33] and it was considered also in [30, 34]. It associates the stability of discrete FO system described by state equation (11) to the asymptotic stability of its approximated solution given by (15).

Definition 5. (The practical stability)
The fractional order system described by (11) is practically stable if its finite dimensional solution (15) is asymptotically stable.

An additional assumption about the positivity of the system (11) allows to apply the simple practical stability conditions given by [30, 34].

Here the Theorems 3 and 5 from paper [30] are employed.

Theorem 1. (Necessary and sufficient practical stability condition of positive system (11) for fixed memory length L)
The positive, FO system (11) with order $0 < \alpha < 1$ is practically stable iff the standard positive system:

$$x(k+1) = (P^+ + \sum_{l=2}^{L} A_l)x(k). \tag{18}$$

is asymptotically stable.

Theorem 2. (Necessary and sufficient practical stability condition of positive system (11)) independently on memory length)
The positive FO system (11) with order $0 < \alpha < 1$ is practically stable for each memory length L iff the standard positive system:

$$x(k+1) = (A^+ + I)x(k). \tag{19}$$

is asymptotically stable.

Both above theorems will be used to stability analysis of the proposed model. This is presented in the next section.

Finally recall the final value thoerem (FVT). It allows to obtain a steady-state value of a time function described by the Laplace or the "z" transform. It is given beneath.

Theorem 3. (Final value theorem for continuous time) Let $f(t)$ is a function of time t and $F(s)$ is its Laplace transform. Assume that $F(s)$:

1) has no poles in the right part of the complex plane,
2) has maximally one pole on the imaginary axis: $s = 0$.

Then:

$$\lim_{t\to\infty} f(t) = \lim_{s\to 0} sF(s). \tag{20}$$

Theorem 4. (Final value theorem for discrete time)
Let $f^+(k)$ is a discrete function of time, defined in k time moments and $F^+(z)$ is its z-transform. Assume that $F^+(z)$:

1) has no poles outside the unit circle,
2) has maximally one pole on the unit circle: $z = 1$.

Then:

$$\lim_{k\to\infty} f^+(k) = \lim_{z\to 1}(z-1)F^+(z). \tag{21}$$

3. THE CONSIDERED HEATING SYSTEM AND ITS TIME-CONTINUOUS, FO MODEL

The heating system is shown simplified in Fig. 1. This is the PCB plate with the flat electric heater, denoted by H. Its coordinates are described by x_{h1}, x_{h2}, y_{h1} and y_{h2} respectively. The temperature of the whole PCB is monitored using an industrial thermal imaging camera, the location and size of measurement area are configurable. The size of camera sensor is $X_s \times Y_s$ pixels ($X_p > Yp$). During further considerations all lengths in the model will be defined relatively with respect to X_p:

$$X = 1, \qquad Y = \frac{X_p}{Y_p}. \tag{22}$$

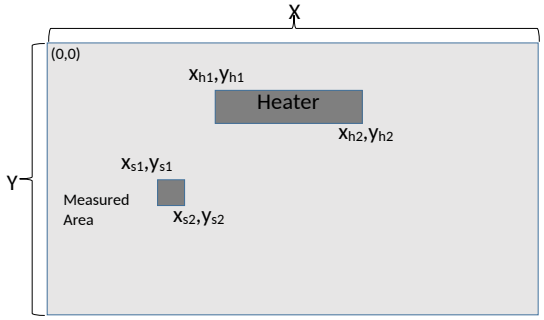

Fig. 1. The experimental system

The area of measurement is marked as S and its coordinates are denoted by x_{s1}, x_{s2}, y_{s1} and y_{s2} respectively. More details about this experimental system are given in the section "Simulations and experiments". The heater and sensor functions are expressed by the simple rectangular functions:

$$b(x,y) = \begin{cases} 1, & x,y \in H, \\ 0, & x,y \notin H, \end{cases} \tag{23}$$

$$c(x,y) = \begin{cases} 1, & x,y \in S, \\ 0, & x,y \notin S. \end{cases} \tag{24}$$

The time-continuous, FO model of the considered system is presented with details in the papers [19, 20, 35]. Here recall its crucial elements, necessary to present of main results.

The FO heat transfer equation takes the following form:

$$\begin{cases} {}_0^C D_t^\alpha Q(x,y,t) = a_w \left(\dfrac{\partial^\beta Q(x,y,t)}{\partial x^\beta} + \dfrac{\partial^\beta Q(x,y,t)}{\partial y^\beta} \right) \\ \qquad -R_a Q(x,y,t) + b(x,y)u(t), \\ \dfrac{\partial Q(0,y,t)}{\partial x} = 0, \quad t \geq 0, \\ \dfrac{\partial Q(X,y,t)}{\partial x} = 0, \quad t \geq 0, \\ \dfrac{\partial Q(x,0,t)}{\partial y} = 0, \quad t \geq 0, \\ \dfrac{\partial Q(x,Y,t)}{\partial y} = 0, \quad t \geq 0, \\ Q(x,y,0) = Q_0, \quad 0 \leq x \leq X, \ 0 \leq y \leq Y \\ y(t) = k_0 \int\limits_0^X \int\limits_0^Y Q(x,y,t)c(x,y)\,\mathrm{d}x\,\mathrm{d}y. \end{cases} \tag{25}$$

In (25) $\alpha > 0$ and $\beta > 0$ denote fractional orders of derivatives with respect to time and length, $a_w > 0$, $R_a \geq 0$ are coefficients of heat conduction and heat exchange, k_0 is a steady-state gain of the model, $b(x,y)$ and $c(x,y)$ are heater and sensor shaping functions, described by (23) and (24).

The heat equation (25) can be expressed as an infinite dimensional state equation:

$$\begin{cases} {}_0^C D_t^{\alpha} Q(t) = AQ(t) + Bu(t), \\ y(t) = CQ(t), \end{cases} \tag{26}$$

where:

$$\begin{aligned} AQ &= a_w \left(\frac{\partial^{\beta} Q(x,y)}{\partial x^{\beta}} + \frac{\partial^{\beta} Q(x,y)}{\partial y^{\beta}} \right) - R_a Q(x,y), \\ D(A) &= \{ Q \in H^2(0,1) : Q'(0) = 0, \\ &\qquad Q'(X) = 0,\ Q'(Y) = 0 \}, \\ a_w,\ R_a &> 0, \\ CQ(t) &= \langle c, Q(t) \rangle,\ \ Bu(t) = bu(t). \end{aligned} \tag{27}$$

The state vector $Q(t)$ takes the following form:

$$Q(t) = \left[q_{0,0},\ q_{0,1},\ q_{0,2} \ldots,\ q_{1,1},\ q_{1,2}, \ldots \right]^T. \tag{28}$$

The state operator A is as follows:

$$\begin{aligned} A = \operatorname{diag} \{ &\lambda_{0,0},\ \lambda_{0,1},\ \lambda_{0,2},\ \ldots,\ \lambda_{1,1},\ \lambda_{1,2},\ \ldots, \\ &\lambda_{2,1},\ \lambda_{2,2}\ \ldots,\ \lambda_{m,n},\ \ldots \}. \end{aligned} \tag{29}$$

The shape of the heated plant (thin metallic surface) suggests assuming the homogenous Neumann boundary conditions. Consequently the eigenfunctions and the eigenvalues take the following form:

$$w_{m,n}(x,y) = \begin{cases} 1, & m,n = 0, \\ \dfrac{2Y}{\pi n} \cos \dfrac{n\pi y}{Y}, & m = 0,\ n = 1,2,\ldots \\ \dfrac{2X}{\pi m} \cos \dfrac{m\pi x}{X}, & n = 0,\ m = 1,2,\ldots \\ \dfrac{2}{\pi} \dfrac{1}{\left(\dfrac{m^{\beta}}{X^{\beta}} + \dfrac{n^{\beta}}{Y^{\beta}} \right)^{\frac{1}{\beta}}} & \\ \times \cos \dfrac{m\pi x}{X} \cos \dfrac{n\pi y}{Y}, & m,\ n = 1,2,\ldots \end{cases} \tag{30}$$

$$\lambda_{m,n} = -a_w \left[\frac{m^{\beta}}{X^{\beta}} + \frac{n^{\beta}}{Y^{\beta}} \right] \pi^{\beta} - R_a, \quad m,\ n = 0,1,2,\ldots \tag{31}$$

The main difference to the one dimensional heat transfer equation is that the eigenvalues (31) can be multiple. The analysis of existence of multiple eigenvalues is discussed in the paper [19].

The control operator takes the following form [19]:

$$B = \left[b_{0,0},\ b_{0,1},\ \ldots,\ b_{1,0},\ b_{1,1},\ \ldots \right]^T. \tag{32}$$

where:

$$b_{m,n} = \langle H, w_{m,n} \rangle = \int_0^X \int_0^Y b(x,y) w_{m,n}(x,y)\, \mathrm{d}x\, \mathrm{d}y. \tag{33}$$

Taking into account (30) we obtain:

$$b_{m,n} = \begin{cases} (x_{h2} - x_{h1})(y_{h2} - y_{h1}), & m,\ n = 0, \\ \dfrac{1}{h_{yn}} (x_{h2} - x_{h1}) a_{nhy}, & \\ \qquad m = 0,\ n = 1,2,3,\ldots, & \\ \dfrac{1}{h_{xm}} (y_{h2} - y_{h1}) a_{mhx}, & \\ \qquad n = 0,\ m = 1,2,3,\ldots, & \\ \dfrac{k_{m,n}}{h_{xm} h_{yn}} a_{mhx} a_{nhy} & \\ \qquad m,\ n = 1,2,3,\ldots \end{cases} \tag{34}$$

where:

$$h_{xm} = \frac{m\pi}{X}, \quad h_{yn} = \frac{n\pi}{Y}, \tag{35}$$

$$k_{m,n} = \frac{2}{\pi} \frac{1}{\sqrt[\beta]{\dfrac{m^{\beta}}{X^{\beta}} + \dfrac{n^{\beta}}{Y^{\beta}}}}, \tag{36}$$

$$\begin{aligned} a_{mhx} &= \left(\sin(h_{xm} x_{h2}) - \sin(h_{xm} x_{h1}) \right), \\ a_{nhy} &= \left(\sin(h_{yn} y_{h2}) - \sin(h_{yn} y_{h1}) \right). \end{aligned} \tag{37}$$

The output operator is as beneath [19]:

$$C = \left[c_{0,0},\ c_{0,1},\ \ldots,\ c_{1,0},\ c_{1,1},\ \ldots \right], \tag{38}$$

where:

$$c_{m,n} = \langle S, w_{m,n} \rangle = \int_0^X \int_0^Y c(x,y) w_{m,n}(x,y)\, \mathrm{d}x\, \mathrm{d}y. \tag{39}$$

In (39) each element $c_{m,n}$ is expressed analogically, as (34):

$$c_{m,n} = \begin{cases} (x_{s2} - x_{s1})(y_{s2} - y_{s1}) & m,n = 0, \\ \dfrac{1}{h_{yn}} (x_{s2} - x_{s1}) a_{nsy} & \\ \qquad m = 0,\ \ n = 1,2,3,\ldots, & \\ \dfrac{1}{h_{xm}} (y_{s2} - y_{s1}) a_{msx} & \\ \qquad n = 0,\ \ m = 1,2,3,\ldots, & \\ \dfrac{k_{m,n}}{h_{xm} h_{yn}} a_{msx} a_{nsy} & \\ \qquad m,\ n = 1,2,3,\ldots \end{cases} \tag{40}$$

In (40) $h_{xm,yn}$ are expressed by (35) and:

$$\begin{aligned} a_{msx} &= (\sin(h_{xm}x_{s2}) - \sin(h_{xm}x_{s1}))\,, \\ a_{nsy} &= \left(\sin(h_{yn}y_{s2}) - \sin(h_{yn}y_{s1})\right). \end{aligned} \tag{41}$$

The dynamic system expressed by (29)–(39) is infinte-dimensional. This implies that its explicit form cannot be employed in modeling and requires applying of a finite dimensional approximation. Such an approximation is obtained via truncation of further modes of the decomposed model at $M \times N$-th place (see [19]). In such a situation the state vector has the dimension $M \times N$ and operators A, B and C turn to matrices of suitable size. The values of M and N ensuring the satisfactory accuracy of the model can be estimated numerically or analytically.

3.1. The step and impulse responses of the model

The step response of the model we obtain using spectrum decomposition property. It takes the following form (see [19]):

$$y_\infty(t) = \sum_{m=0}^{\infty}\sum_{n=0}^{\infty} y_{m,n}(t), \tag{42}$$

where m,n-th mode of response is as follows:

$$y_{m,n}(t) = \frac{E_\alpha(\lambda_{m,n}t^\alpha) - 1(t)}{\lambda_{m,n}} b_{m,n}c_{m,n}. \tag{43}$$

In (43) $E_\alpha(..)$ is the one parameter Mittag-Leffler function, $\lambda_{m,n}$, $b_{m,n}$ and $c_{m,n}$ are expressed by (31), (33) and (39) respectively.

During simulations the finite-dimensional sum needs to be employed:

$$y_{MN}(t) = \sum_{m=0}^{M}\sum_{n=0}^{N} y_{m,n}(t). \tag{44}$$

The analysis of the external positivity requires the knowledge of an impulse response of a system. It can be computed analogically as the step response, using the decomposition of the spectrum of the system.

The impulse response for a single mode of the system (26)-(39) is as follows:

$$g_{m,n}(t) = t^{\alpha-1}E_{\alpha,\alpha}\left(\lambda_{m,n}t^\alpha\right) b_{m,n}c_{m,n}\,, \tag{45}$$

where $E_{\alpha,\alpha}(..)$ is the two-parameter Mittag-Leffler function, the rest of parameters are the same as in (43).

Consequently the impulse response and its finite-dimensional approximation are as beneath:

$$g_\infty(t) = \sum_{m=0}^{\infty}\sum_{n=0}^{\infty} g_{m,n}(t), \tag{46}$$

$$g_{MN}(t) = \sum_{m=0}^{M}\sum_{n=0}^{N} g_{m,n}(t), \tag{47}$$

where $g_{m,n}(t)$ are the single modes expressed by (45).

The accuracy of both approximated responses (44) and (47) is determined by the size of model expressed by M and N. The convergence of the model is discussed in the paper [20]. The accuracy for the one-dimensional case was discussed in the conference presentation [12].

4. MAIN RESULTS

4.1. The discrete FOBD model of the thermal system

The discrete model is obtained analogically as in the one-dimensional case (see [16] and [36]). During further considerations the upper index "+" denotes the discrete-time system. The matrices (12) and (13) of the discrete state equation (11) takes the following form:

$$\begin{aligned} A^+ &= \mathrm{diag}\{\lambda^+_{0,0},..,\lambda^+_{m,n}\}, \\ B^+ &= h^\alpha B, \\ C^+ &= C, \end{aligned} \tag{48}$$

where:

$$\lambda^+_{m,n} = h^\alpha \lambda_{m,n}. \tag{49}$$

This yields the following form of the matrix (16) in the solution of discrete state equation (15):

$$P^+ = diag\{P^+_{0,0},\ldots,P^+_{M,N}\}. \tag{50}$$

where:

$$P^+_{m,n} = \lambda^+_{m,n} + \alpha. \tag{51}$$

Consequently the model (26) takes the discrete form (11):

$$\begin{cases} (\Delta^\alpha_L Q^+)(k+1) = A^+Q^+(k) + B^+u^+(k), \\ y^+(k) = C^+Q^+(k). \end{cases} \tag{52}$$

The solution of the discrete system (52) takes the form as (15):

$$Q^+(k+1) = P^+Q^+(k) - \sum_{l=2}^{L} A^+_l Q^+(k-l) + B^+u^+(k), \tag{53}$$

where P^+, B^+ and A^+_l are expressed by (50), (17) and (13) respectively.

To the analysis of the stability the free solution, starting from initial condition is more convenient. It is as follows:

$$Q^+(k+1) = P^+Q^+(k) - \sum_{l=2}^{L} A^+_l Q^+(k-l). \tag{54}$$

Next the elementary properties of the model: decomposition of the system, positivity, stability and convergence need to be discussed. The fundamental difference to the one-dimensional system discussed previously is that two orders M and N describing both spatial coordinates need to be considered.

4.2. The decomposition of the system

The state vector $Q^+(k)$ of the discrete model (15) can be expressed as:

$$Q^+(k) = \begin{bmatrix} q^+_{0,0}(k) \\ \dots \\ q^+_{M,N}(k) \end{bmatrix}. \tag{55}$$

The matrices P^+ and A^+_l describing the solution of the discrete system (53) are diagonal matrices. Consequently this solution can be decomposed into MN independent modes, associated to m,n-th state variable $Q^+_{m,n}(k)$ and described by the m,n-th eigenvalue. The multiple of eignevalues, possible for two-dimensional case does not matter.

The m,n-th mode of free solution for fixed memory length L takes the form as follows:

$$q^{+L}_{m,n}(k+1) = \lambda^+_{m,n} q^+_{m,n}(k) - \sum_{l=2}^{L} d_l q^+_{m,n}(k-l), \quad m = 0,\dots,M, \;\; n = 0,\dots,N. \tag{56}$$

The m,n-th mode of the forced response to control signal $u^+(k)$ is as beneath:

$$y^{+L}_{m,n}(k) = c^+_{m,n}\left(q^{+L} + b^+_{m,n}u^+(k)\right), \quad m = 0,\dots,M, \;\; n = 0,\dots,N. \tag{57}$$

With each mode of solution (56) the following characteristic polynomial $w_{m,n}(z^{-1})$ is associated:

$$w^L_{m,n}(z^{-1}) = 1 - \lambda^+_{m,n} z^{-1} + \sum_{l=2}^{L} d_l z^{-l}. \tag{58}$$

Using the forced solution (57) for the m,n-th mode the transfer function $G^L_{m,n}(z^{-1})$ between its input and output can be given:

$$G^L_{m,n}(z^{-1}) = \frac{c^+_{m,n} b^+_{m,n} z^{-1}}{1 - z^{-1}\lambda^+_{m,n} + \sum_{l=2}^{L} d_l z^{-l}}, \quad m = 1,\dots,M, \;\; n = 1,\dots,N. \tag{59}$$

The standard system (18) for the m,n-th mode is as follows:

$$v^L_{m,n}(k+1) = \left(P^+_{m,n} + \sum_{l=2}^{L} A_l\right) v^L_{m,n}(k). \tag{60}$$

For each memory length the free solution takes the following form:

$$q^{+\infty}_{m,n}(k+1) = \lambda^+_{m,n} q^+_{m,n}(k) - \sum_{l=2}^{\infty} d_l q^+_{m,n}(k-l), \quad m = 0,\dots,M, \;\; n = 0,\dots,N. \tag{61}$$

The m,n-th mode of the forced response is as beneath: The m,n-th mode of the forced response to control signal $u^+(k)$ is as beneath:

$$y^{+\infty}_{m,n}(k) = c^+_{m,n}\left(q^{+\infty} + b^+_{m,n}u^+(k)\right), \quad m = 0,\dots,M, \;\; n = 0,\dots,N \tag{62}$$

and analogically the characteristic polynomial, transfer function and standard system are following:

$$w^\infty_{m,n}(z^{-1}) = 1 - \lambda^+_{m,n} z^{-1} + \sum_{l=2}^{\infty} d_l z^{-l}, \tag{63}$$

$$G^\infty_{m,n}(z^{-1}) = \frac{c^+_{m,n} b^+_{m,n} z^{-1}}{1 - z^{-1}\lambda^+_{m,n} + \sum_{l=2}^{\infty} d_l z^{-l}}, \quad m = 1,\dots,M, \;\; n = 1,\dots,N, \tag{64}$$

$$v^\infty_{m,n}(k+1) = (\lambda^+_{m,n} + 1) v^\infty_{m,n}(k). \tag{65}$$

Using (57) or (62) with $u^+(k) = 1(k)$ allows us to calculate the step response of the discrete system (52):

$$y^{+L,\infty}(k) = \sum_{m=0}^{M}\sum_{n=0}^{N} y^{+L,\infty}_{m,n}(k). \tag{66}$$

The decomposition of the model presented above will be also applied to analyze of basic properties of model: internal positivity, practical stability, accuracy and convergence. This is shown in the next subsections.

4.3. The positivity

The brief analysis of the positivity is necessary to apply the stability conditions formulated by Remarks 1 and 2.

In the beginning it is important to note that the stability is determined by the behaviour of the state $Q^+(k)$ only. An input and an output of the system, described by the operators B and C are not required to analyse. It can be at once noted that the state operator A of the time continuous system (29), (31) is the Metzler matrix (definition of the Metzler matrix is given e.g. in [30]). This implies that the time-continuous state of the system under consideration is positive and asymptotically stable.

Next the positivity of the system after discretization described by (48) and (49) should be tested. To do it the simple positivity condition given as equation (6) in the paper [30] can be employed. It is as follows:

$$P^+ \in \mathbb{R}^+. \tag{67}$$

Operator P^+ expressed by (50) is diagonal. This implies that the condition (67) turns to the following form:

$$\forall\, m = 0,..,M, \; \forall n = 0,..N \;\; P^+_{m,n} > 0. \tag{68}$$

After application of (49) in (68) we obtain the following condition, possible to numerical tests for given set of parameters:

$$\forall\, m = 0,..,M,\ \forall n = 0,..,N:$$
$$a_w\left(\left(\frac{m\pi}{X}\right)^{\beta}+\left(\frac{n\pi}{Y}\right)^{\beta}\right) < \frac{\alpha}{h^{\alpha}} - R_a\,. \tag{69}$$

Parameters presented e.g. in the paper [20] allow to conclude that the condition (69) should be met in big part of real situations.

4.4. The practical stability

The time-continuous model of the heat transfer is stable due to "natural" stability of this process. But wrong values of sample time h or memory length L can cause the loss of the stability of a discrete-time model. The presented stability analysis gives guidance to proper selecting of these parameters to avoid problems with a stability of the proposed model.

The stability conditions for the one-dimensional model using FOBD have been proposed in the paper [16] and recalled by the paper [36]. The fundamental result of stability was that too high order N of the one-dimensional discrete model can cause its instability.

Here these results need to be adopted to the two-dimensional case.

Notice that the practical stability or instability for the whole considered system is determined by the asymptotic stability or instability of its separated modes (56) or (61). This is described by the following remarks.

Remark 1. (The practical stability of the discrete, decomposed FO system)

The discrete non-integer order system (52) will be practically stable for fixed memory length L iff each mode of its solution (56) is asymptotically stable.

The discrete non-integer order system (52) will be practically stable for each memory length L if and only if each mode of its solution (61) is asymptotically stable.

Remark 2. (The instability of the discrete, decomposed FO system)

The discrete non-integer order system (52) will be unstable for fixed memory length L iff there exists at least one unstable mode of its solution (56).

The discrete non-integer order system (52) will be unstable for each memory length L iff there exists at least one instable mode of its solution (61).

The practical stability can be explicitly tested using both above remarks. This requires examining the localisation of roots of each characteristic polynomial (58) for $m = 1,..,M, n = 1,\ldots,N$. The degree of each polynomial is equal to $L+1$. It makes us use numerical methods only and can be done with the use of MATLAB. On the other hand it allows us to test the correctness of analytical condition obtained using the standard systems (60) and (65).

The decomposition of state equation and possibility of stability testing by investigation of MN seperated, scalar, internally positive systems allows us to formulate analytical stability conditions. To do it the conditions (18) and (19) will be employed.

In practical application of the proposed model important is to give the dependence of its stability on dimensions M, N, memory length L and sample time h. Here the approach presented in the papers [16] and [36] will be used. The main complication is caused by two dimensions of the model: M and N. To avoid it assume that both dimensions are equal: $M = N$.

The maximum dimension $N^{L,\infty}$ assuring the stability of the model is described by the following propositions:

Proposition 1. (The maximum dimension of the model N^L for fixed memory length L)

Consider the discrete model (48)–(54). Assume that it meets the assumption about internal positivity (69).

The maximum dimension N_L of the model for fixed memory length L assuring its stability is as follows:

$$N^L < \frac{XY}{\pi}\left(\frac{S_H}{X^{\beta}+Y^{\beta}}\right)^{\frac{1}{\beta}}, \tag{70}$$

where:

$$D_L = \sum_{l=2}^{L} d_l\,,$$
$$S = \frac{\alpha + D_L - h^{\alpha}R_a}{h^{\alpha}a_w}\,, \tag{71}$$
$$S_H = S + \frac{1}{h^{\alpha}a_w}\,.$$

For each memory length the maximum dimension N^{∞} is described as follows:

Proposition 2. (The maximum dimension of the model N^{∞} for each memory length)

Consider the discrete model (48)–(54). Assume that it meets the assumption about internal positivity (69).

The maximum dimension N_{∞} of the model for each memory length assuring its stability is as follows:

$$N^{\infty} < \frac{XY}{\pi}\left(\frac{S_{\infty}}{X^{\beta}+Y^{\beta}}\right)^{\frac{1}{\beta}}, \tag{72}$$

where:

$$S_{\infty} = \frac{2 - h^{\alpha}R_a}{h^{\alpha}a_w}\,. \tag{73}$$

Comparing conditions (70) vs (72) it can be observed that the second is the limit case for the first one.

4.5. The accuracy

The accuracy ϵ of the proposed discrete model will be analyzed analogically as in the one dimensional case given in [13,17,36]. It is defined as the difference between steady-state response of the time-continuous system (25) y_{ss} and discrete system (52) y^{+}_{ss} to the Heaviside function $1(t)$. For fixed and each memory length (denoted by ∞) it is expressed as follows:

$$\epsilon^{L,\infty} = |y_{ss}| - |y^{+L,\infty}_{ss}|, \tag{74}$$

where upper indices $^{L,\infty}$ denote the fixed and each memory length respectively.

The steady state response of the time-continuous system is as follows:

$$y_{ss} = CA^{-1}B, \tag{75}$$

where A, B and C there are state, input and output matrices of the system respectively. With respect to (29), (32) and (38) it turns to the following form:

$$y_{ss} = \sum_{m=0}^{M}\sum_{n=0}^{N}\frac{b_{m,n}c_{m,n}}{\lambda_{m,n}}, \tag{76}$$

where $\lambda_{m,n}$, $b_{m,n}$ and $c_{m,n}$ are expressed by (31), (34) and (40) respectively.

The steady-state responses for the discrete system can be computed using final value theorem (21). Using it to (59) and (64) yields:

$$y_{ss}^{+L} = \sum_{m=0}^{M}\sum_{n=0}^{N}\frac{b_{m,n}^{+}c_{m,n}^{+}}{1-\lambda_{m,n}^{+}+D_L}, \tag{77}$$

$$y_{ss}^{+L} = \sum_{m=0}^{M}\sum_{n=0}^{N}\frac{b_{m,n}^{+}c_{m,n}^{+}}{2-\lambda_{m,n}^{+}}, \tag{78}$$

where $b_{m,n}^{+}$, $c_{m,n}^{+}$, $\lambda_{m,n}^{+}$ and D_L are described by (48), (49) and (71) respectively. It can be observed that:

$$y_{ss}^{+\infty} = \lim_{L\to\infty} y_{ss}^{+L}. \tag{79}$$

The accuracy (74) as a function of orders M and N can be estimated numerically using (76) and (77) or (78). This is presented in the next section.

4.6. The convergence

The convergence will be analyzed analogically as in the one-dimensional case [36]. The rate of convergence (ROC) is defined as the absolute value of the steady-state response of the m, n-th mode, expressed as follows:

$$ROC_{m,n}^{L} = \left|\frac{b_{m,n}^{+}c_{m,n}^{+}}{1-\lambda_{m,n}^{+}+D_L}\right|, \tag{80}$$

$$ROC_{m,n}^{\infty} = \left|\frac{b_{m,n}^{+}c_{m,n}^{+}}{2-\lambda_{m,n}^{+}}\right|. \tag{81}$$

In practice it is important to know minimum orders of model M, N assuring required value of ROC. Such a condition can be given for equal both orders: $M = N$. It is formulated as the following proposition:

Proposition 3. (The minimum orders M and N assuring the predefined value of ROC)

Consider the discrete model (48)–(54),

Assume that both orders of the model are equal: $M = N$ and required ROC is equal Δ.

The minimum dimension N^{Δ} of the model for fixed memory length L assuring the predefined $ROC = \Delta$ is given by the following inequality:

$$N^{\Delta} > \left(\frac{h^{\alpha}P}{\Delta}\right)^{\frac{1}{6}}, \tag{82}$$

where:

$$P = \frac{64(XY)^2}{\pi^6\left(X^{-\beta}+Y^{-\beta}\right)^{\frac{2}{\beta}}}. \tag{83}$$

Proof. The condition $ROC < \Delta$ is expressed as:

$$\left|\frac{b_{m,n}^{+}c_{m,n}^{+}}{1-\lambda_{m,n}^{+}+D_L}\right| < \Delta. \tag{84}$$

With respect to (13), (14), (37) and (41) for $M = N > 0$ the expression $b_{m,n}^{+}c_{m,n}^{+}$ can be estimated as follows:

$$b_{m,n}^{+}c_{m,n}^{+} \le 16h^{\alpha}\left(\frac{k_{m,n}}{h_{xm}h_{yn}}\right)^2. \tag{85}$$

In further considerations the absolute value $|..|$ can be omitted due to the estimation (85) and the denominator of (84) are always positive. The coefficients $k_{m,n}$, $h_{x,m}$ and $h_{y,n}$ are expressed by (35) and (36). This yields:

$$P = \left(\frac{k_{m,n}}{h_{xm}h_{yn}}\right)^2, \tag{86}$$

where P is expressed by (83).

Next recall the form of the eigenvalue $\lambda_{m,n}^{+}$ and introduce the following symbols:

$$\begin{aligned} R_6 &= D_L + 1 + h^{\alpha}R_a, \\ R_{\beta} &= h^{\alpha}a_w\pi^{\beta}\left(X^{-\beta}+Y^{-\beta}\right). \end{aligned} \tag{87}$$

Using (86) and (87) in (84) yields:

$$\begin{aligned} &\frac{h^{\alpha}P}{N^6(R_6+R_{\beta}N^{\beta})} < \Delta \iff \\ &\iff \frac{h^{\alpha}P}{\Delta} < N^6(R_6+R_{\beta}N^{\beta}). \end{aligned} \tag{88}$$

For real, identified parameters of the model the coefficients (87) can be estimated as: $R_6 \approx 1$ and $R_{\beta} \approx 0$. This gives:

$$\frac{h^{\alpha}P}{N^6} < \Delta \iff \frac{h^{\alpha}P}{\Delta} < N^6 \iff \left(\frac{h^{\alpha}P}{\Delta}\right)^{\frac{1}{6}} < N, \tag{89}$$

The use of $N = N^{\Delta}$ in (89) gives directly the condition (82) and the proof is completed. □

The above condition is "cautious" due to use of all proposed simplifications. It can be applied together with the stability condition (70) to estimate the range of orders ensuring both practical stability and required convergence of the model. This will be shown in the next section.

5. SIMULATIONS AND EXPERIMENTS

5.1. The construction of the experimental system

The experimental system is shown in Fig. 2. The size of the measuring field expressed in pixels are equal: $X_p = 380$, $Y_p = 290$. The PCB is heated by the flat electric heater 170×20 pixels, attached in points: $x_{h1} = 100$, $y_{h1} = 40$. The maximum power of this heater equals to 10 W. The temperature of the metallic surface is read with the use of thermal camera OPTRIS PI 450, connected to computer via USB and installed dedicated software OPTRIS PI CONNECT. The range of measured temperature is 0–250°C, the sampling frequency is 80 Hz. The control signal to heater is sent from computer via NI LabView, NI MyRIO and amplifier. The maximum current from amplifier equals to 400 [mA] and with a voltage of 12 V gives the maximum power 4.8 W. The PCB plate is not isolated from the environment. This implies that measurements are strongly dependent on ambient temperature. The presented experiments were done in hot summer. During experiments only basic filtering assured by camera software was sufficient (see Fig. 4). The goal of the experiments was to obtain the step response. The "zero" level denotes the heater switched off, the "one" level is the full power of the heater. The temperature fields for both states are shown in Fig. 3. This figure shows also the points of measurement of the step response, marked as "Area 1–4". Areas 1–3 are located in different places of the PCB, area 4 describes the mean temperature of the whole heater. Coordinates of all places of measurement are given in Table 1. All step responses are collected in Fig. 4. During calculations all coordinates $x_{..}$ and $y_{..}$ are used in the relative form according to (22).

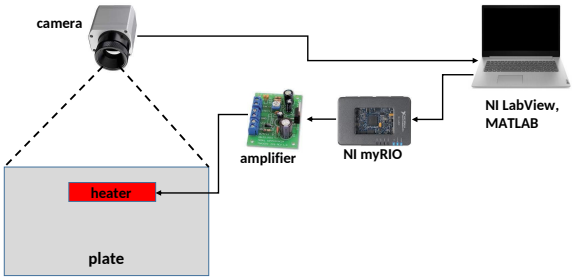

Fig. 2. The construction of the experimental system

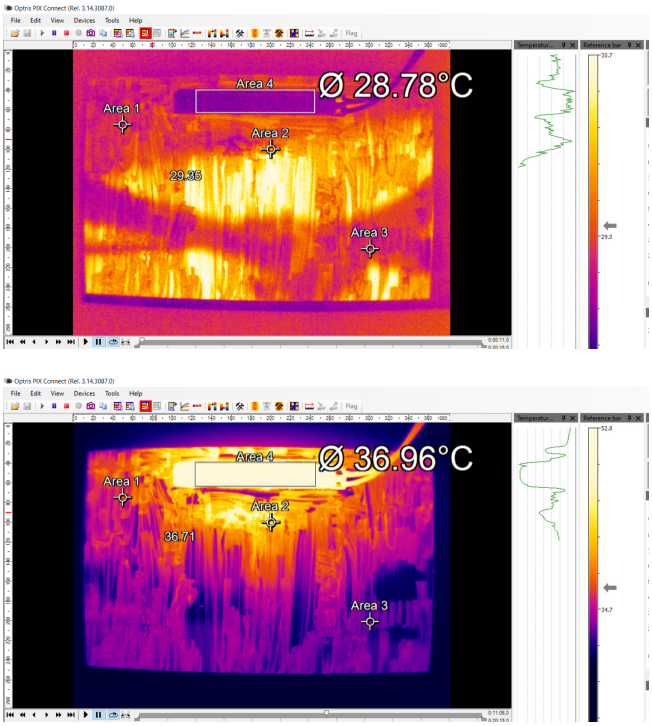

Fig. 3. The steady-state temperature fields for nonheated (top) and heated plate (bottom). The temperature strongly depends on ambient temperature. The colour scale in each case is different

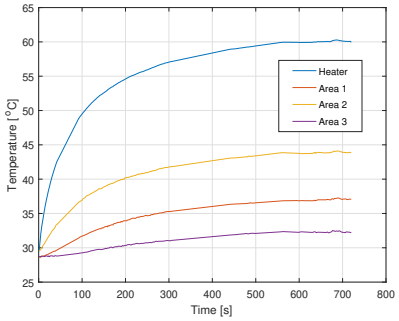

Fig. 4. The step responses of temperature in all tested fields

Table 1
Coordinates of measuring areas (in pixels)

area	x_{s1}	y_{s1}	x_{s2}	y_{s2}
1	50	75	52	77
2	200	100	202	102
3	300	200	302	202
4	120	40	250	60

5.2. The identification of the model

To identify of both orders of the model α, β and its parameters describing the heat transfer and exchange: a_w and R_a the known cost function IAE was applied. Its discrete version takes the following form:

$$IAE = \frac{1}{K_f} \sum_{k=1}^{K_f} \left| y^+(k) - y_e(k) \right|. \tag{90}$$

where $y^+(k)$ is the step response of the discrete model (52), computed using (66), $y_e(k)$ is the experimental step response and K_f is the amount of samples.

The parameters of the model were identified via numerical minimization of this function with the use of MATLAB function *fminsearch*. This function was used because the step responses presented in Fig. 4 are rather smooth. Results for all tested areas are given in Tables 2–5. Comparison of step responses of model vs experiments is shown in Fig. 5. Step responses presented in this figure were computed with the use of data marked by (F) in the tables.

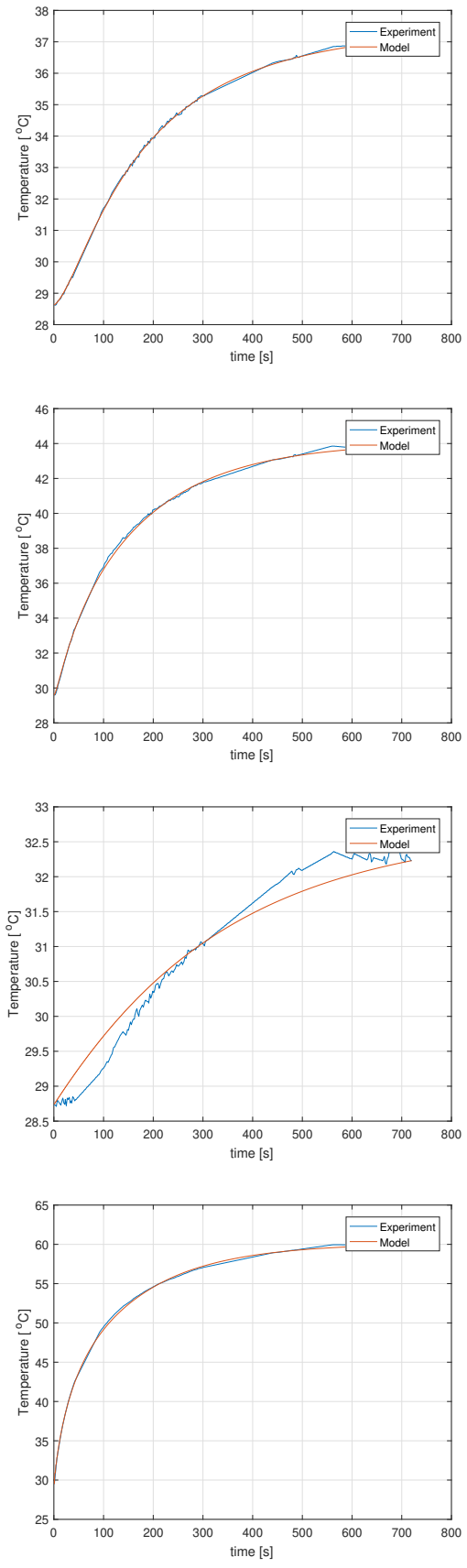

Fig. 5. Step responses of model $y^+(k)$ vs experiments for all areas. Parameters of each model are marked by (F) in Tables 2–5. Experimental responses are marked in blue, responses of the model are marked in red

Table 2
Identified parameters of the model – area 1

L	M,N	α	β	a_w	R_a	IAE
100	3	0.9986	3.1803	0.0017	0.0100	0.0561
100	5	0.9994	2.2933	0.0021	0.0106	0.0716
100	7	0.8188	0.0000	0.0061	0.0156	0.0875
200	3	1.0004	2.9121	0.0024	0.0100	0.0566
200	5	0.9976	2.7013	0.0007	0.0111	0.0838
200	7 (F)	0.9954	2.3994	0.0001	0.0090	0.0396

Table 3
Identified parameters of the model – area 2

L	M,N	α	β	a_w	R_a	IAE
100	3	0.9936	2.7149	0.0013	0.0114	0.1123
100	5	0.7392	0.0000	0.0017	0.0155	0.1517
100	7	0.7354	0.0000	0.0007	0.0149	0.1506
200	3	0.8866	1.5793	0.0014	0.0140	0.1223
200	5 (F)	0.8656	1.3517	0.0074	0.0154	0.1023
200	7	0.8290	1.4826	-0.0000	0.0183	0.1313

Table 4
Identified parameters of the model – area 3

L	M,N	α	β	a_w	R_a	IAE
100	3	0.9980	2.7340	0.0021	0.0059	0.2110
100	5 (F)	0.9981	0.8586	0.0020	0.0060	0.2085
100	7	0.7029	2.0866	0.0014	0.0056	0.1606
200	3	0.9993	3.0075	0.0018	0.0059	0.2106
200	5	0.9993	0.0011	0.0004	0.0058	0.2151
200	7	0.5750	2.3299	0.0006	0.0374	0.5963

Table 5
Identified parameters of the model – area 4

L	M,N	α	β	a_w	R_a	IAE
100	3	0.0823	1.3325	0.0103	0.5895	0.3547
100	5	0.5385	1.7443	0.0019	0.0010	0.2983
100	7	0.5045	1.6037	0.0028	0.0069	0.2974
200	3	0.6873	0.0006	0.0774	0.0301	0.2321
200	5 (F)	0.7789	0.0012	0.0643	0.0216	0.1867
200	7	0.7319	1.8458	0.0023	0.0263	0.2409

The analysis of Tables 2–5 and diagrams 5 allows us to conclude that the quality of the model in the sense of the cost function (90) is strongly determined by the point of measurement: it is the best for area 1, and weak for the area 3. Simultaneously, the good accuracy is obtained for relatively low orders of model M, N and memory length L.

Interesting observation is the value of the order β for area 4, described by row (F) in Table 5. Its value, close to zero points that in this place (heater) the distributed-parameter model reduces to the lumped parameter model.

5.3. Practical stability

The condition of the practical stability (70) can be examined using parameters described in the previous section. As an example consider the parameters given in the row (F) in Table 3. The sample time was equal: $h = 1\,[s]$. The use of conditions (70) and (72) gives the upper estimation of maximum orders assuring the practical stability of the model. They are equal: $N^L < 9.2516$ and $N^\infty < 10.2969$.

Next for all modes $m, n = 0, \ldots, N, N$ roots of all characteristic polynomials (58) and roots of all standard systems (60) were numerically computed for two values of M, N: "stable": $M = N = 8$ and "unstable": $M = N = 15$. Results are illustrated by Figs. 6 and 7. The main conclusion about the practical stability of the considered model is that the increasing of orders M, N leads to loss of stability. This is analogical to the one-dimensional case (see [16, 36]). This results directly from (31) and (12). For the time-continuous model increasing of orders M, N moves eigenvalues left in the complex plane, but for the discrete time this causes the "migration" of eigenvalues outside of the unit circle. Next, the increasing of the memory length L allows to a little bit increase the maximum value of orders, but this causes a significant increase in computational complexity with a slight improvement in accuracy (see next subsection).

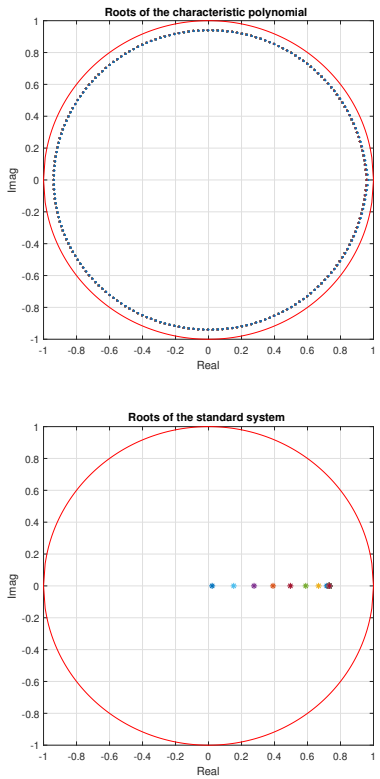

Fig. 6. Roots of characteristic polynomials and standard systems for "stable" dimensions of model: $M = N = 8$

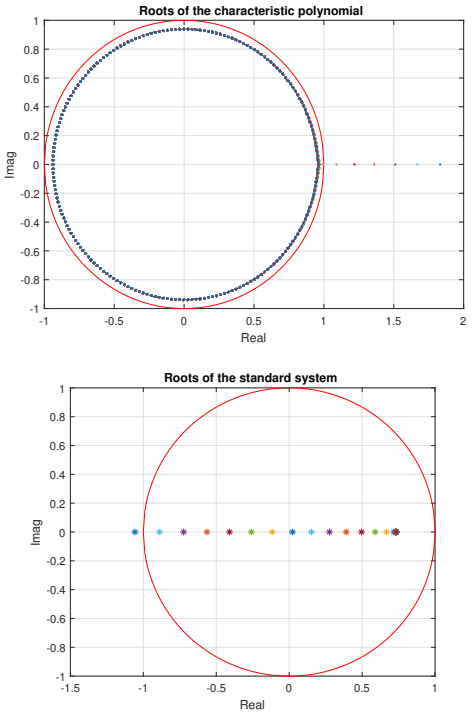

Fig. 7. Roots of characteristic polynomials and standard systems for "unstable" dimensions of model: $M = N = 15$

5.4. Accuracy and convergence

The accuracy was tested for the worst case, appearing in area 3. To tests the parameters from row (F) in Table 4 were used. The accuracy (74) as a function of orders M and N is shown in Fig. 8. The diagram 8 allows to conclude that the accuracy of the proposed discrete model does not depend on the memory length L, but it is determined by the dimensions of model M and N. Next, for both orders greater than 7 the improvement in accuracy is slight.

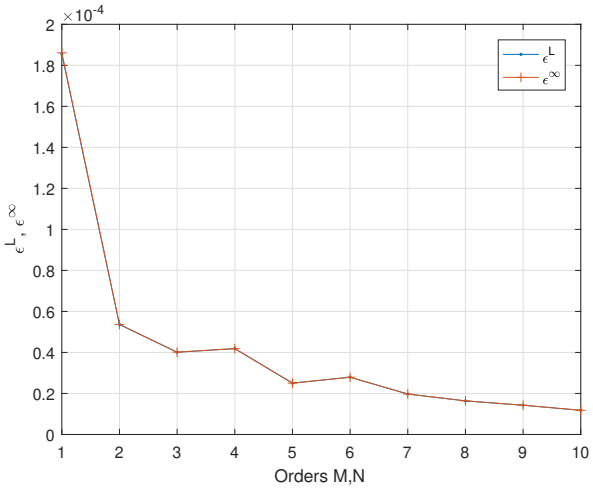

Fig. 8. Accuracy (74) for area 3, $L = 100$ and each memory length

The convergence of the proposed model was tested using relations (80) and (81). The ROC as a function of the number

of mode for fixed and each memory lenghts are shown in Fig. 9. Calculations were done using parameters of the model from row (F) in Table 2.

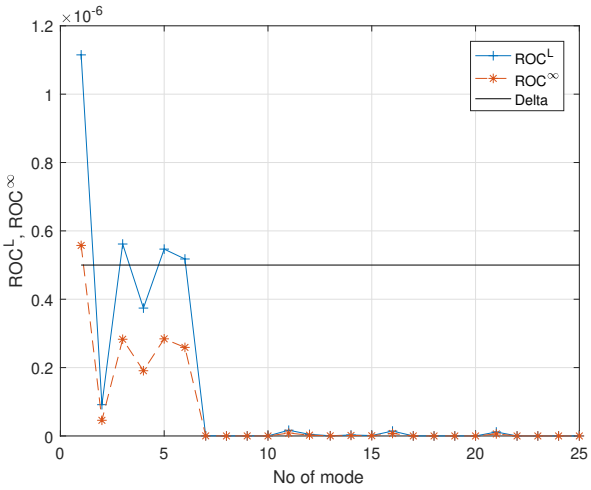

Fig. 9. Rate of Convergence for area 1, $M = N = 7$, $L = 200$ and each memory length and the required value Δ

Next consider the required value of ROC equal $\Delta = 5e-07$. The use of condition (82) gives the minimum value of both orders $N^{\Delta} > 5.6289$. This is also illustrated by Fig. 9.

From Fig. 9 it can be also concluded that the convergence of the proposed model is stronger determined by the orders of the model M, N than by the memory length L. For each memory length the ROC is a little bit smaller than for fixed memory length, but for orders greater than 7 the the difference is negligible.

Summarizing, the use of both conditions of practical stability and convergence allows to obtain the permissible range of orders M, N of the model. These orders lie in the interval $[N^{\Delta}; N^{L}]$. For the conisdered numerical example this is the interval: $[5.6289; 9.2516]$ and really gives the values of M, N from 6 to 9.

6. FINAL CONCLUSIONS

The main conclusion from the paper is that the proposed, discrete time, fractional order model can properly describe thermal processes in the two-dimensional thin metallic surface. The good accuracy in the sense of the IAE cost function is achieved for low orders of the model and relatively short memory length L.

The proposed conditions of stability and convergence are contradictory, because the better convergence requires the increasing of orders, what leads to instability of the model. However, both condtions applied together allow to obtain precise estimation of orders allowing to keep both stability and good convergence.

The spectrum of the further investigations of the presented issue is broad. It covers u.a. analysis of the numerical complexity of the proposed model as well as its verification with the use of various experimental data.

An another important issue is to consider the uncertainty of the parameters of the model, because such a situation is typical during use of thermal imaging cameras.

Next, the identification of the model can be also done using biologically inspired methods, e.g. Particle Swarm Optimization (PSO) or Grey Wolf Optimization (GWO).

Finally, the internal and external positivity of this model need also be analysed.

ACKNOWLEDGEMENTS

This paper was sponsored by AGH UST project no 16.16. 120.773.

REFERENCES

[1] I. Podlubny, *Fractional Differential Equations*. San Diego: Academic Press, 1999.

[2] S. Das, *Functional Fractional Calculus for System Identification and Controls*. Berlin: Springer, 2010.

[3] A. Dzieliński, D. Sierociuk, and G. Sarwas, "Some applications of fractional order calculus," *Bull. Pol. Acad. Sci. Tech. Sci.*, vol. 58, no. 4, pp. 583–592, 2010.

[4] R. Caponetto, G. Dongola, L. Fortuna, and I. Petras, "Fractional order systems: Modeling and Control Applications," in *World Scientific Series on Nonlinear Science*, L.O. Chua, Ed. Berkeley: University of California, 2010, pp. 1–178.

[5] C. Gal and M. Warma, "Elliptic and parabolic equations with fractional diffusion and dynamic boundary conditions," *Equat. Control Theory*, vol. 5, no. 1, pp. 61–103, 2016.

[6] E. Popescu, "On the fractional cauchy problem associated with a feller semigroup," *Math. Rep.*, vol. 12, no. 2, pp. 181–188, 2010.

[7] D. Sierociuk, T. Skovranek, M. Macias, I. Podlubny, I. Petras, A. Dzielinski, and P. Ziubinski, "Diffusion process modeling by using fractional-order models," *Appl. Math. Comput.*, vol. 257, no. 1, pp. 2–11, 2015.

[8] J. F. Gómez, L. Torres, and R. Escobar, "Fractional derivatives with Mittag-Leffler kernel. trends and applications in science and engineering," in *Studies in Systems, Decision and Control, vol. 194*, J. Kacprzyk, Ed. Switzerland: Springer, 2019, pp. 1–339.

[9] A. Boudaoui, Y. E. hadj Moussa, Hammouch, and S. Ullah, "A fractional-order model describing the dynamics of the novel coronavirus (covid-19) with nonsingular kernel," *Chaos Solitons Fractals*, vol. 146, p. 110859, 2021.

[10] M. Farman, A. Akgül, S. Askar, T. Botmart, A. Ahmad, and H. Ahmad, "Modeling and analysis of fractional order zika model," *AIMS Math.*, vol. 7, no. 3, pp. 3912–3938, 2022.

[11] K. Oprzędkiewicz, E. Gawin, and W. Mitkowski, "Modeling heat distribution with the use of a non-integer order, state space model," *Int. J. Appl. Math. Comput. Sci.*, vol. 26, no. 4, pp. 749–756, 2016.

[12] K. Oprzędkiewicz, E. Gawin, and W. Mitkowski, "Parameter identification for non integer order, state space models of heat plant," in *MMAR 2016: 21th International Cconference on Methods and Models in Automation and Robotics*, Międzyzdroje, Poland, 2016, pp. 184–188.

[13] K. Oprzedkiewicz, R. Stanislawski, E. Gawin, and W. Mitkowski, "A new algorithm for a cfe approximated solution of a discrete-time non integer-order state equation," *Bull. Pol. Acad. Sci. Tech. Sci.*, vol. 65, no. 4, pp. 429–437, 2017.

[14] K. Oprzędkiewicz, W. Mitkowski, and E. Gawin, "An accuracy estimation for a non integer order, discrete, state space model of heat transfer process," in *Automation 2017: innovations in automation, robotics and measurment techniques*, Warsaw, Poland, 2017, pp. 86–98.

[15] K. Oprzędkiewicz, W. Mitkowski, E. Gawin, and K. Dziedzic, "The caputo vs. caputo-fabrizio operators in modeling of heat transfer process," *Bull. Pol. Acad. Sci. Tech. Sci.*, vol. 66, no. 4, pp. 501–507, 2018.

[16] K. Oprzędkiewicz and E. Gawin, "The practical stability of the discrete, fractional order, state space model of the heat transfer process," *Arch. Control Sci.*, vol. 28, no. 3, pp. 463–482, 2018.

[17] K. Oprzędkiewicz and W. Mitkowski, "A memory efficient non integer order discrete time state space model of a heat transfer process," *Int. J. Appl. Math. Comput. Sci.*, vol. 28, no. 4, pp. 649–659, 2018.

[18] K. Oprzędkiewicz, "Non integer order, state space model of heat transfer process using atangana-baleanu operator," *Bull. Pol. Acad. Sci. Tech. Sci.*, vol. 68, no. 1, pp. 43–50, 2020.

[19] K. Oprzędkiewicz, W. Mitkowski, and M. Rosol, "Fractional order model of the two dimensional heat transfer process." *Energies*, vol. 14, no. 19, pp. 1–17, 2021.

[20] K. Oprzędkiewicz, W. Mitkowski, and M. Rosol, "Fractional order, state space model of the temperature field in the pcb plate," *Acta Mech. Automatica*, vol. 17, no. 2, pp. 180–187, 2023.

[21] M. Dlugosz and P. Skruch, "The application of fractional-order models for thermal process modelling inside buildings," *J. Build. Phys.*, vol. 1, no. 1, pp. 1–13, 2015.

[22] M. Ryms, K. Tesch, and W. Lewandowski, "The use of thermal imaging camera to estimate velocity profiles based on temperature distribution in a free convection boundary layer," *Int. J. Heat Mass Transf.*, vol. 165, no. 1, p. 120686, 2021.

[23] H. Khan, R. Shah, P. Kumam, and M. Arif, "Analytical solutions of fractional-order heat and wave equations by the natural transform decomposition method," *Entropy*, vol. 21, no. 21, pp. 597–618, 2019.

[24] L. Olsen-Kettle, *Numerical solution of partial differential equations*. Queensland, Australia: The University of Queensland, 2011.

[25] S.K. Al-Omari, "A fractional fourier integral operator and its extension to classes of function spaces," *Adv. Diff. Equat.*, vol. 1, no. 195, pp. 1–9, 2018.

[26] P. Kulczycki, J. Korbicz, and J. Kacprzyk (eds), *Fractional Dynamical Systems: Methods, Algorithms and Applications*. New Jersey, London, Singapore: Springer, 2022.

[27] T. Kaczorek, "Singular fractional linear systems and electrical circuits," *Int. J. Appl. Math. Comput. Sci.*, vol. 21, no. 2, pp. 379–384, 2011.

[28] T. Kaczorek and K. Rogowski, *Fractional Linear Systems and Electrical Circuits*. Bialystok: Bialystok University of Technology, 2014.

[29] P. Ostalczyk, *Discrete Fractional Calculus. Applications in Control and Image Processing*. New Jersey, London, Singapore: World Scientific, 2016.

[30] M. Buslowicz and T. Kaczorek, "Simple conditions for practical stability of positive fractional discrete-time linear systems," *Int. J. Appl. Math. Comput. Sci.*, vol. 19, no. 2, pp. 263–269, 2009.

[31] D. Mozyrska and E. Pawluszewicz, "Fractional discrete-time linear control systems with initialisation," *Int. J. Control*, vol. 1, no. 1, pp. 1–7, 2011.

[32] T. Kaczorek, "Reachability of cone fractional continuous time linear systems," *Int. J. Appl. Math. Comput. Sci.*, vol. 19, no. 1, pp. 89–93, 2009.

[33] T. Kaczorek, "Practical stability of positive fractional discrete-time systems,," *Bull. Pol. Acad. Sci. Tech. Sci.*, vol. 56, no. 4, pp. 313–317, 2008.

[34] A. Ruszewski, "Practical and asymptotic stability of fractional discrete-time scalar systems described by a new model," *Arch. Control Sci.*, vol. 26, no. 4, pp. 441–452, 2016.

[35] K. Oprzędkiewicz, K. Dziedzic, and W. Mitkowski, "Accuracy analysis of the fractional order, positive, state space model of heat transfer process," in *MMAR 2021 : 25th international conference on Methods and Models in Automation and Robotics*, Międzyzdroje, Poland, 2021, pp. 325–330.

[36] K. Oprzędkiewicz, K. Dziedzic, and Ł. Więckowski, "Non integer order, discrete, state space model of heat transfer process using Grünwald-Letnikov operator," *Bull. Pol. Acad. Sci. Tech. Sci.*, vol. 67, no. 5, pp. 905–914, 2019.